Preliminary Assessment of a Solar Absorption System for Air Conditioning Applications

J.C. Jiménez-García, W. Rivera

Instituto de Energías Renovables, Universidad Nacional Autónoma de México, Temixco, Morelos, México.

Abstract

A low-capacity solar absorption system for air conditioning applications has been developed. The system uses the mixture ammonia-lithium nitrate and plate heat exchangers as the main components. Several experimental test runs were carried out at different operating conditions for the generator, condenser and absorber. The system achieved an internal cooling power close to 3.1 kW, with cooling temperatures around 6 °C and an internal coefficient of performance around 0.62.

Key-words: absorption cooling system, solar air conditioning, ammonia-lithium nitrate

1. Introduction

In the last years absorption systems have gained increasing interest by the fact that they can be operated with either solar thermal energy or residual heat from industries. Around 15% of the electricity produced worldwide is used for air-conditioning and cooling (Statistics, I. E. A., 2011), so absorption systems may help to reduce this percentage. Currently, the research on absorption systems has focused in three main aspects:

(i) the study of alternative mixtures,
(ii) the development of more efficient and low cost components, and
(iii) the development of advanced systems

Up to now, several studies have been carried out on the development of absorption cooling prototypes operating with ammonia-water (Jakob et al., 2008) and water/lithium bromide (Achuthan et al., 2011; Agyenim et al., 2010; González-Gil et al., 2011; Lizarte et al., 2012, 2013; Qu et al., 2010; Venegas et al., 2011; Yin et al., 2013;). These two mixtures have been the most used since they possess great advantages. However due to their well-known drawbacks, Best and Rivera (2015) presented a review of thermal cooling systems. According to their study, the ammonia-lithium nitrate mixture possesses some advantages over the conventional ones. Regarding ammonia-lithium nitrate mixtures, some of the most relevant studies are cited below. Rivera et al. (2012) and Moreno-Quintanar et al. (2012) reported the assessment of an intermittent solar absorption refrigeration system operating with NH_3-$LiNO_3$ using a cylindrical parabolic collector as a generator–absorber. The results showed that it was possible to produce up to 8 kg of ice per day. Generation temperatures varied from 75 °C to 110 °C achieving evaporation temperatures as low as -11 °C and solar coefficients of performance of 0.08. Llamas et al. (2007, 2014) reported the results of a 10 kW solar absorption air conditioning system for a cooling capacity between 5 and 10 kW operating with the ammonia-lithium nitrate mixture. The system was air cooled and the heat was supplied by evacuated solar collectors. Coefficients of performance up to 0.53 were achieved with chilled water temperatures as low as 0 °C. Hernández-Magallanes et al. (2014) reported the experimental assessment of an absorption cooling system operating with the ammonia-lithium nitrate mixture. The generator and absorber were helical coil falling film heat exchangers while condenser, evaporator and economizer were plate heat exchangers (PHE). The COP values varied between 0.45 and 0.7 while the cooling capacity was between 0.52 to 2.52 kW, for generator temperatures between 85 °C and 105 °C and condenser temperatures from 18 °C to 36 °C. Zamora et al. (2014, 2015) reported two studies on the assessment of an absorption chiller operating with the ammonia-lithium nitrate mixture using compact heat exchangers as the main components. The authors reported that the water-cooled

doi:10.18086/swc.2017.28.11 Available at http://proceedings.ises.org

prototype yields 12.9 kW of cooling capacity and an electrical COP of 19.3, when operating at 15 ºC for chilled water, 90 ºC for heating water and 35 ºC for cooling water. Dominguez-Inzunza et al. (2016) carried out the evaluation of an ammonia/lithium nitrate absorption cooling system. The generator temperatures varied between 80 °C and 100 °C, while the cooling water temperatures varied from 20 °C to 34 °C. Cooling capacities up to 4.5 kW and evaporator temperatures as low as 4 °C were achieved with coefficients of performance ranging from 0.3 to 0.62.

On the other hand, regarding to the use of PHE as components in absorption cooling systems, some of the most relevant works are the following: Goyal et al. (2017) reported the evaluation of a small-capacity, waste-heat driven ammonia-water absorption chiller. The system developed used waste heat from diesel generator exhaust to desorb the refrigerant solution. The system was designed to deliver 2.71 kW of cooling at extreme ambient temperature of 51.7 °C obtaining a coefficient of performance of 0.55. The system utilizes air-cooled finned-tube in the absorber and condenser and microchannel array in the evaporator. Experiments were carried out at ambient temperatures of 29.7–44.2 °C, delivered cooling duties of 2.54–1.91 kW. Zacarías et al. (2013) reported the results on the experimental assessment of the adiabatic absorption of ammonia vapor in an ammonia-lithium nitrate solution using a fog jet nozzle. The system utilizes compact heat exchangers in all the components with exception of the absorber. The authors reported that the approach to adiabatic equilibrium factor for the conditions essayed was always between 0.82 and 0.93. Khan et al. (2012a, 2012b) carried out an experimental investigation on evaporation heat transfer and pressure drop for ammonia in 30º and 60º chevron PHE. The experiments were performed for saturation temperatures ranging from 25 ºC to 2 ºC and the heat flux varied between 21 kW m^{-2} and 44 kW m^{-2}. The experimental results showed a significant effect of saturation temperature, heat and exit vapor quality on heat transfer coefficient and pressure drop. The authors proposed correlations for the Nusselt number and friction factor. Stasiek (1998) carried out experimental studies of heat transfer and fluid flow across corrugated-undulated heat exchanger surfaces. The authors used a true color image processing of liquid crystal images for temperature and heat transfer distribution measurements in six element-shapes of heat exchangers. The authors reported that the technique could be of considerable use in improving the design of all types of plate heat exchangers. Ibarra-Bahena et al. (2015) reported the experimental results of a single stage heat transformer using PHE in all its main components. The system operated with the water-carrol mixture. The experimental gross temperature lift achieved values from 18.5 to 22.2 ºC and the coefficients of performance varied from 0.30 to 0.35.

From the literature review it can be seen that just a few prototypes have been developed using the ammonia-lithium nitrate mixture and only the research carried out by Zamora et al. (2014, 2015) involves plate heat exchangers as main components. However, their studies only present some global results for the coefficients of performance for very specific conditions and they did not do a parametric study in order to evaluate the system's performance under several operating conditions. Therefore, this paper presents the evaluation of a single-stage absorption cooling system operating with the ammonia-lithium nitrate mixture at different temperatures heating and cooling water.

2. System description

2.1 Experimental setup

The absorption system proposed consists of the following components: generator, absorber, condenser, evaporator, economizer, pump, throttle device, and a couple of tanks. The system was operated with the ammonia-lithium nitrate mixture, and it was built using five plate heat exchangers (PHE) as the main components which were oriented in vertical configuration. The PHE utilized in the system were manufactured by *Alfa Laval*, and it was considered the model *Alfanova 52* for generator, economizer and absorber, the number of plates for each heat exchanger is 40, for condenser and evaporator the model *Alfanova 27* was chosen with 20 plates in each heat exchanger. A *Milton Roy* diaphragm pump with a nominal power of 745 W was used in order to pumping the working fluid from the absorber to the generator. The throttle device used was a stainless steel low-pressure metering valve coupled with vernier handle, which has a maximum flow

coefficient equal to 0.004. Besides, a couple of tanks with a volume capacity near to 2 liters were included in the system: one of them is located at the exit of the generator, whose function is to enable the phases' separation, thus it allows the ammonia vapor flow to the condenser and the liquid solution flow to the absorber. On the contrary, the second tank acts as a mixing chamber, because the solution with a low refrigerant's concentration (weak solution) that comes from the generator and the solution that is being recirculated get mixed there. The system's measures are: 1.06 x 1 x 0.65 meters (front-height-depth). All the components utilized in the system are 100% stainless steel, in order to avoid their degradation caused by ammonia and lithium nitrate. The described components can be seen in the system's schematic diagram shown in figure 1.

Although the aim of the system is to be driven by solar energy, in order to perform the experimental assessment under controlled conditions, up to now, the experimental tests were carried out using three auxiliary systems. The thermal energy required to separate the refrigerant from the working mixture is supplied to the generator by means of an auxiliary heating system. This auxiliary system uses an electric resistance to heating up a mass flow rate of water, the hot water is supplied to the generator at a gauge pressure near to 200 kPa (2 bar), thus, avoiding the boiling of the water at generation temperatures.

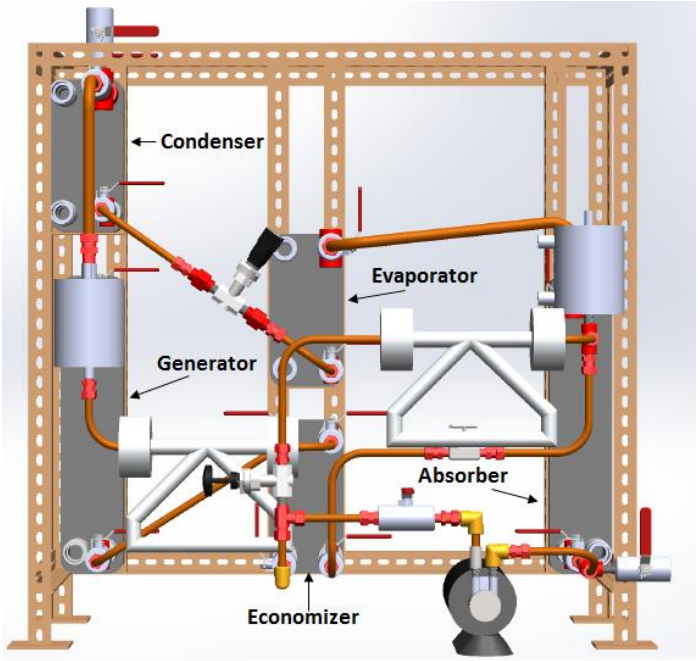

Fig. 1: Schematic diagram of the absorption cooling machine

On the other hand, the thermal power removed from the condenser and absorber is dissipated by means of an auxiliary cooling system, this cooling system consists of a storage tank, a recirculating water pump and a commercial chiller. Once the flow of water has removed heat from the condenser and absorber, its temperature is reduced in the chiller, transferring the heat to the ambient air, when the water leaves the chiller it is stored in the tank, the recirculating pump takes the low-temperature water from the storage tank and pumps it to the condenser and absorber, hence, the water is able to take thermal energy from the condenser and absorber again. The third auxiliary system is intended to supply a mass flow rate of water to the evaporator, in order to be cooled by the absorption system. This system also has a storage tank, a pump and an electric resistance, and it was designed to provide the heat necessary to keep the water's temperature constant.

2.2 Operation of the system

A mass flow rate of hot water is supplied to the generator in order to get the ammonia and the solution separated. The two phase mixture (ammonia vapor and weak solution) leaves the generator and enters to a separation tank, there, the ammonia vapor flows to the condenser where it is liquefied by means of the cooling water supplied by the chiller. The ammonia in liquid phase, leaves the condenser and goes through the

expansion valve, reducing its pressure and temperature. Once the ammonia has passed through the valve, its thermodynamic state is a saturated liquid-vapor mixture and its temperature is the lowest temperature of the entire cycle. Under these conditions, the ammonia mixture enters into the evaporator extracting a thermal load from the water circulating in the adjacent channels of the PHE as a countercurrent flow, producing the system's cooling effect. The ammonia leaves the evaporator as superheated vapor and goes to the absorber where it is mixed with the weak solution coming from the generator. This mixture process releases thermal energy, which is transferred to the cooling water that flows in the absorber. Finally, the solution with high concentration of refrigerant (strong solution) leaving the absorber is pumped to the generator starting the cycle again.
Furthermore, an economizer is included in the system, whose purpose is to exchange heat between the solution flows going to and leaving the generator, in order to enhance the coefficient of performance (COP) by reducing the heat rejection in the absorber as well as the heat supplied to the generator.

2.3 Instrumentation

In order to evaluate the system's performance while the operative conditions are modified, a set of temperature, pressure and mass flow rate sensors were included in the absorption system. The pressure in the system was measured in the generator, condenser, evaporator and absorber. *Ashcroft* piezoelectric transducers were utilized. Regarding the mass flow rates in the absorption system: two types of sensors were considered: in order to obtain the refrigerant produced and the weak solution mass flow rates, a couple of *Micro Motion Elite Coriolis Flow Meters* was used. The strong solution as well as the external mass flow rates of water were registered by several turbine flow meters. The temperature for each current was measured at the inlet and outlet ports in every PHE. Every measuring device used for the system's experimental assessment was calibrated and a set of calibration equations was obtained. Each outlet signal was received, processed and stored by a *HP* data acquisition system using the software *Agilent VEE Pro 9.3*, were the equations obtained were utilized in order to find the expected values. The sensors' position in the system is shown in the schematic diagram presented in figure 2.

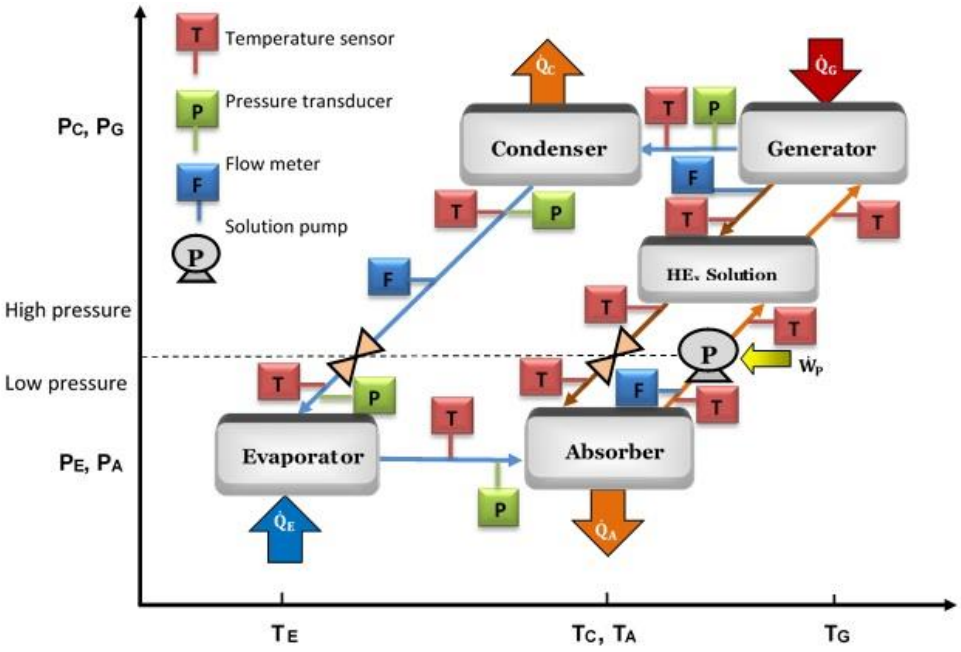

Fig. 2: Schematic diagram showing the sensors location in the absorption cooling machine

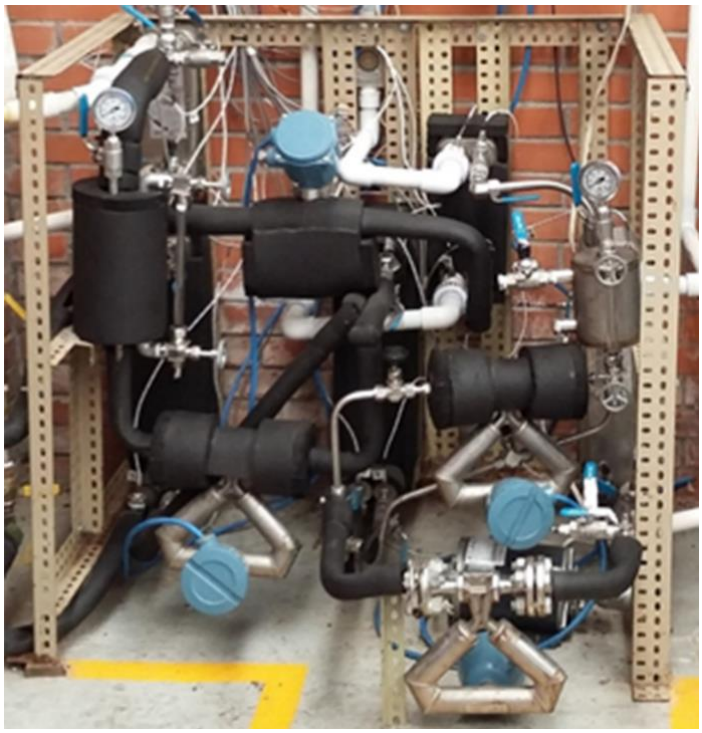

Fig. 3: Developed absorption cooling machine

The uncertainties associated to the cited instrumentation are presented in Table 1.

Tab. 1: Instruments uncertainties

Measuring instrument	Uncertainty
Elite Coriolis flowmeter	± 0.10%
Omega rotameter	± 1%
Turbine flowmeter	± 1%
Pressure transducer	± 1%
RTD sensor	± 0.3°C

3. Main equations

The coefficient of performance is a measure of the system's efficiency and it can be determined based on internal or external parameters. Internal parameters are related to the conditions for the weak and strong solutions and the refrigerant produced. External parameters are influenced by the conditions of the mass flow rates of heating and chilled water, at inlet and outlet of the generator and evaporator, respectively, as well as the work supplied by the related pumps.

The internal coefficient of performance (COP_{int}) can be determined by equation 1:

$$COP_{int} = \frac{\dot{Q}_{e,int}}{\dot{Q}_{g,int} + \dot{W}_{b,int}} \qquad \text{(eq. 1)}$$

In equation 1 $\dot{Q}_{e,int}$ represents the system's cooling power, this term is the thermal power transferred to the ammonia in the evaporator and it is calculated as shown in equation 2.

$$\dot{Q}_{e,int} = \dot{m}_{ref}(h_{e,o} - h_{e,i}) \quad \text{(eq. 2)}$$

On the other hand, the term $\dot{Q}_{g,int}$ represents the actual heat power supplied to the strong solution in the generator, it is calculated as an energy balance considering the mass flow rates across the PHE. The energy balance calculation can be advertised in equation 3.

$$\dot{Q}_{g,int} = \dot{m}_{weak}(h_{g,o-weak}) + \dot{m}_{ref}(h_{g,o-NH3}) - \dot{m}_{strong}(h_{g,i}) \quad \text{(eq. 3)}$$

The term $\dot{W}_{b,int}$ in equation 1 expresses the mechanical power supplied to the system in order to pump the strong solution from the absorber to the generator. It is determined calculating the enthalpies difference (before and after the pump) for the strong solution mass flow rate. Equation 3 exposes the manner in which the mechanical power for the internal pump is determined.

$$\dot{W}_{b,int} = \dot{m}_{strong}(h_{ec,i-strong} - h_{a,o}) \quad \text{(eq. 4)}$$

The properties for the ammonia-lithium nitrate mixture were calculated using the equations reported by Farshi et al. (2014). The ammonia properties were determined from the *REFPROP* software using the international institute of refrigeration (IIR) reference state.

4. Results

In order to assess the absorption cooling system, approximately 40 test runs have been carried out. A parametric analysis was performed with the aim of demonstrating the effects of the change in a parameter on the others. Thus, the condensation temperature was varied while parameters as the strong solution mass flow rate and temperatures of heating water and water to be chilled, were kept constant. The working mixture employed in the experimental assessment had an ammonia's mass concentration equal to 54 % and it was kept constant for the test runs presented.

The preliminary assessment was performed for generation temperatures between 80 and 95 °C, and condensation temperatures from 22 °C to 32 °C. Generation temperature was varied in 5 °C increments. The condensation temperature steps were equivalent to 2 °C.

For each test run steady state conditions were achieved and kept by a minimum period of 30 minutes. The figures 4 to 7 present the temperature profiles obtained in the main components for a chosen test run, where the generation temperature was 80 °C while the condensation temperature was 28 °C. The mass flow rate values utilized for the system's assessment are presented in table 2.

Tab. 2: Mass flow rate values for parameters enternal and internal

Parameter	Mass flow rate (kg/s)
Heating water	0.25
Cooling water	0.2
Chilled water	0.183
Solution to generator	0.016

In figure 4 is advertised that generator temperatures are constant for the test's period of time. The highest temperature corresponds to heating water entering to generator (Tg,wi). On the contrary, the lowest temperature is the solution going into the generator (Tg,i), which almost reaches the highest temperature when it leaves the PHE. That means the selected parameters such as solution mass flow rate and flow arrangement (countercurrent arrangement) are adequated for the conditions presented. The average temperatures for the solution entering and leaving the generator are 64.1 °C and 78.2 °C, respectively.

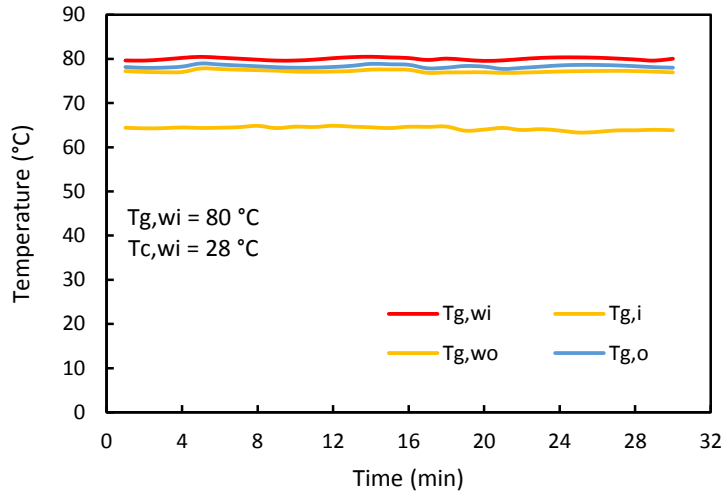

Fig. 4: Temperature profiles in generator during the test run

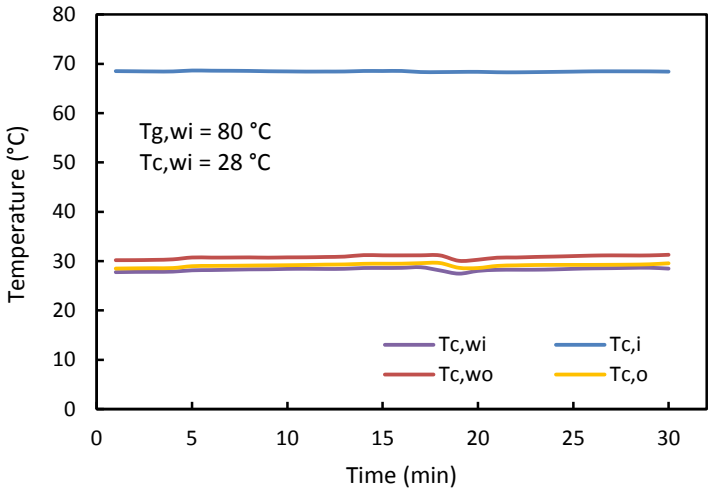

Fig. 5: Temperature profiles in condenser during the test run

In the case of the temperature profiles in condenser, from figure 5 it can be seen the steady state is also kept. The refrigerant enters to the condenser at an average temperature of 68.5 °C ($\mathbf{T_{c,i}}$), and leaves the heat exchanger at an average temperature near to 29.12 °C ($\mathbf{T_{c,o}}$). The pressure measured in this test run is approximated to 1.25 MPa (12.5 bar) which means that for the $\mathbf{T_{c,o}}$ measured it is assured that refrigerant condensation is achieved. In the case of cooling water an average temperatures difference between the inlet and outlet near to 2.6 °C is accomplished.

The profiles for attained temperatures in evaporator are shown in figure 6, where it is possible to observe that for the test conditions, the refrigerant at the inlet's port in evaporator ($\mathbf{T_{e,i}}$) had a temperature near to 10 °C. The water to be chilled ($\mathbf{T_{e,wi}}$) entered the evaporator at an average temperature of 20 °C and experimented a reduction of 2.5 °C in average. It is important to mention the refrigerant temperature leaving the evaporator ($\mathbf{T_{e,o}}$) is very close to $\mathbf{T_{e,wi}}$, this probably means that refrigerant is overheated, which would imply that the mass flow rate of refrigerant produced is low, regarding the evaporator's capacity.

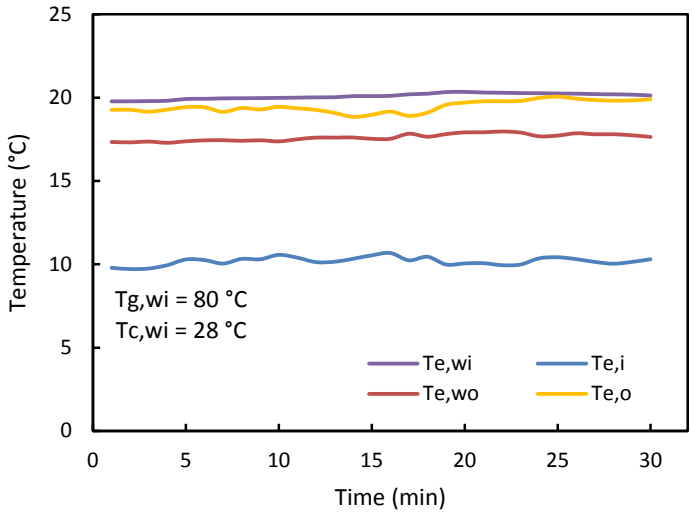

Fig. 6: Temperature profiles in evaporator during the test run

In figure 7 is possible to see the temperature profiles through the absorber. The cooling water entering the PHE has an average temperature of 28 °C ($\mathbf{T}_{a,\mathbf{wi}}$) and leaves it at an average temperature of 30.65 °C ($\mathbf{T}_{a,\mathbf{wo}}$). On the other hand, a two phase mixture of ammonia vapor and weak solution arrives at an average temperature ($\mathbf{T}_{a,\mathbf{i}}$) near to 47 °C. After the absorption process has taken place, the solution with a higher ammonia concentration leaves the absorber at an average temperature approximated to 32.4 °C.

In figures 5 and 7 a temperature perturbation is seen on the water profiles, this disturbance is induced by the auxiliary cooling system which has an intermittent behavior which is determined by the temperature variations in the storage tank. The described disruption causes, at the same time, a disturbance on the exit temperature of the opposite flow, which is reflected on its temperature profile of both PHE: condenser and absorber.

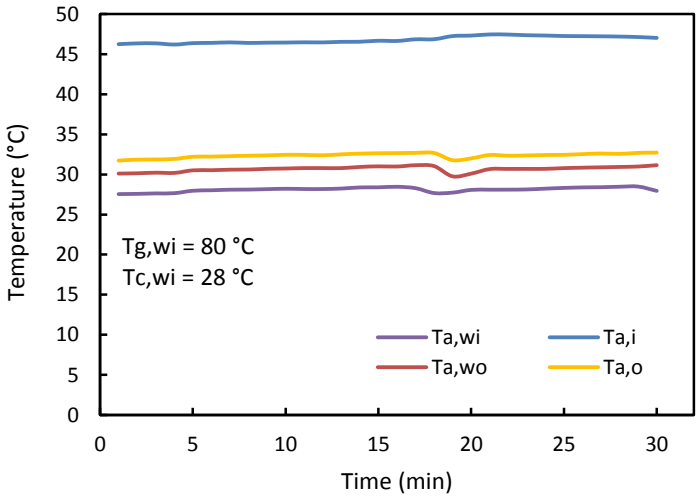

Fig. 7: Temperature profiles in absorber during the test run

The thermal power transferred to ammonia in evaporator (calculated as $\dot{\boldsymbol{Q}}_{\boldsymbol{e,int}}$ from eq. 2) is presented in figure 8. Figure 8 shows the downward trend for this parameter as the condensation temperature grows up. In other words, the system's cooling capacity is reduced at higher condensation temperatures. This fact was expected

because the higher condensation temperatures the higher pressures in the components are gotten, and higher evaporation temperatures for ammonia are obtained, which means the cooling capacity is reduced. The figure 8 also shows a direct relationship between generation temperatures and cooling power, having that the lowest generation temperatures the lowest cooling capacities are attained. When the system was operated at $\mathbf{T_{g,wi}} = \mathbf{95\ °C}$, the pressures attained were very similar to those for $\mathbf{T_{g,wi}} = \mathbf{90\ °C}$, for that reason some key temperatures and thermal powers are very close, as it can be seen in figure 8.

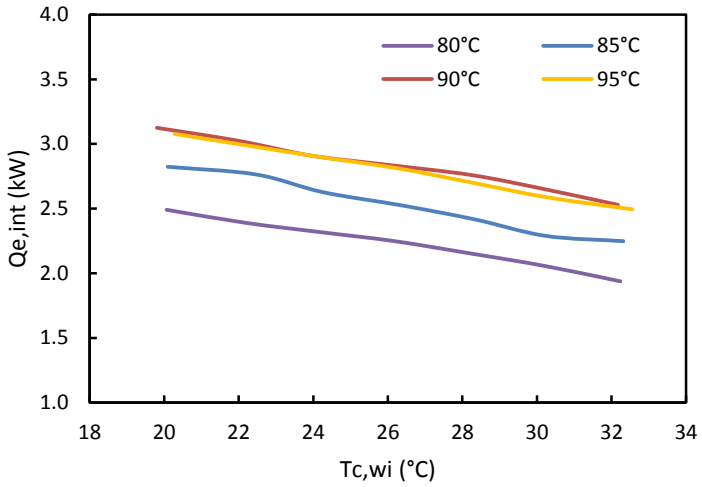

Fig. 8: Internal thermal power transferred in evaporator for several generation temperatures

Figure 9 exhibites the ammonia mass flow rate produced for every generation temperature tested. As condensation temperature increased, the ammonia mass flow rate produced was diminished, presenting a downward linear changement for every trend. On the other side, it could be seen from figure 9 that there is a direct relationship between the generation temperatures and the amount of ammonia circulating throught the condenser and evaporator. Thus, at higher generation temperatures a higher amount of ammonia is produced and a higher cooling effect is obtained as it is demonstrated in figure 8.

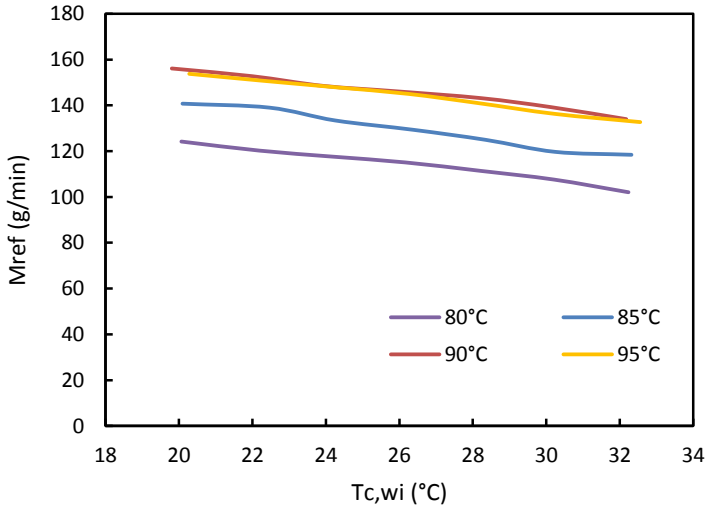

Fig. 9: Refrigerant mass flow rate produced during the assessment

The lowest system's temperature is reached after the ammonia has passed through the throttle valve ($\boldsymbol{T_{e,i}}$), just before the inlet to evaporator. The ammonia temperature was measured at this point and it was plotted in figure 10 against condensation temperature, for each generation temperature considered. As it is presented in figure 10, this temperature augmented as condensation temperature grew up. This was due to the fact that at higher condensation temperatures higher pressures in absorber and evaporator are gotten, which causes the saturation temperature for ammonia to increase.

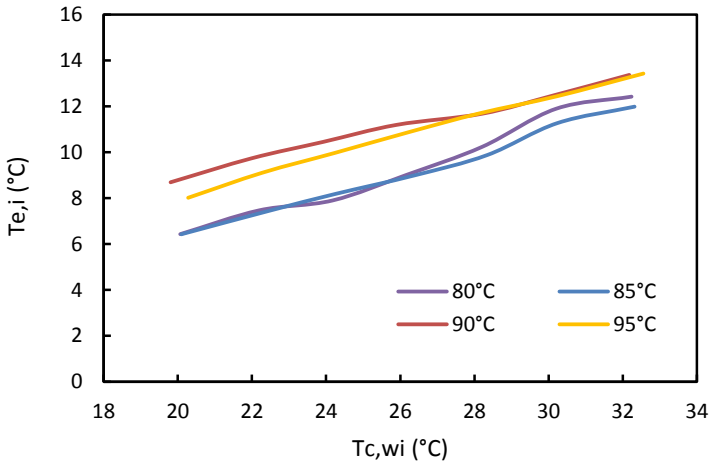

Fig. 10: Ammonia evaporation temperatures registered

The variation of internal COP with respect to condensation temperatures for each generation temperature tested is shown in figure 11. From this figure, it is possible to see that, as a general trend, the internal COP decreases as the condensation temperature increases, besides this, the figure 11 makes evident that for higher generation temperatures, higher coefficients of performance are reached, according to what was expected.

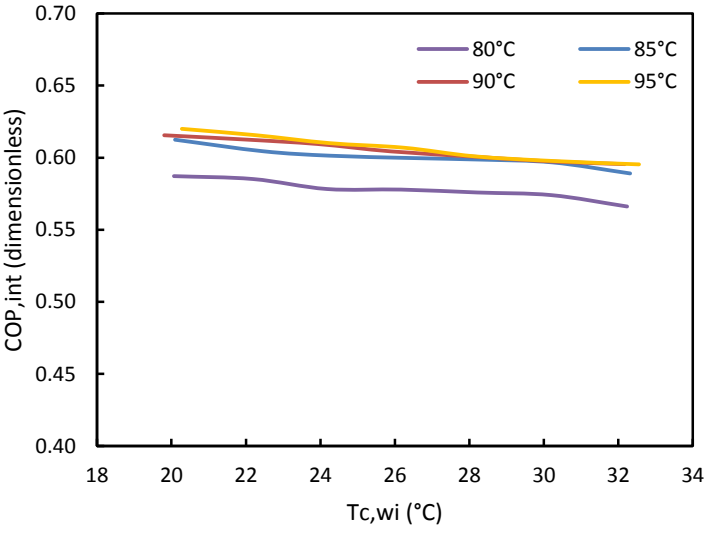

Fig. 11: Internal coefficient of performance for the absorption system

For the lowest $\boldsymbol{T_{g,wi}}$ (80 °C) the highest $\boldsymbol{COP_{int}}$ value was 0.587 when $\boldsymbol{T_{c,wi}}$ was 20 °C, while the minimum COP was 0.566 when 32 °C were kept in condenser. The $\boldsymbol{COP_{int}}$ for $\boldsymbol{T_{g,wi} = 85\ °C}$ varied from 0.612 to 0.589 for the condensation range specified. Regarding 90 and 95 °C generation temperatures, the highest $\boldsymbol{COP_{int}}$ obtained were 0.612 and 0.619 at $\boldsymbol{T_{c,wi} = 20\ °C}$ respectively, while the lowest value was close to 0.595 for both cases.

5. Conclusions

The preliminary assessment of an experimental absorption cooling system operating with the ammonia-lithium nitrate working mixture was presented. The assessment was performed for generation temperatures from 80 to 95 °C, while condensation temperatures were varied from 20 to 32 °C. A mass flow rate of solution going to generator was kept constant at 0.016 kg/s (1 kg/min). Key parameters such as main temperatures, cooling powers, mass flow rates of refrigerant produced and internal coefficients of performance were presented and discussed. It was found the system achieved a cooling power close to 3.1 kW for a generation temperature equal to 90°C. On the other hand, for the lowest generation temperatures, cooling temperatures around 6 °C were attained. A maximum internal coefficient of performance near to 0.62 was obtained when $T_{g,wi} = 95\ °C$ and $T_{c,wi} = 20\ °C$.

6. References

Achuthan, M., Venkataraman, A., & Rathnasamy, R. (2011). Experimental analysis on the performance and characteristics of compact solar refrigeration system. Distributed Generation & Alternative Energy Journal, 26(3), 66-80.

Agyenim, F., Knight, I., & Rhodes, M. (2010). Design and experimental testing of the performance of an outdoor LiBr/H_2O solar thermal absorption cooling system with a cold store. Solar energy, 84(5), 735-744.

Best, R., & Rivera, W. (2015). A review of thermal cooling systems. Applied Thermal Engineering, 75, 1162-1175.

Domínguez-Inzunza, L. A., Hernández-Magallanes, J. A., Soto, P., Jiménez, C., Gutiérrez-Urueta, G., & Rivera, W. (2016). Experimental assessment of an absorption cooling system utilizing a falling film absorber and generator. Applied Thermal Engineering, 103, 1105-1111.

Farshi, L. G., Ferreira, C. I., Mahmoudi, S. S., & Rosen, M. A. (2014). First and second law analysis of ammonia/salt absorption refrigeration systems. *International journal of refrigeration*, *40*, 111-121.

González-Gil, A., Izquierdo, M., Marcos, J. D., & Palacios, E. (2011). Experimental evaluation of a direct air-cooled lithium bromide–water absorption prototype for solar air conditioning. Applied Thermal Engineering, 31(16), 3358-3368.

Goyal, A., Staedter, M. A., Hoysall, D. C., Ponkala, M. J., & Garimella, S. (2017). Experimental evaluation of a small-capacity, waste-heat driven ammonia-water absorption chiller. International Journal of Refrigeration, 79, 89-100.

Hernández-Magallanes, J. A., Domínguez-Inzunza, L. A., Gutiérrez-Urueta, G., Soto, P., Jiménez, C., & Rivera, W. (2014). Experimental assessment of an absorption cooling system operating with the ammonia/lithium nitrate mixture. Energy, 78, 685-692.

Ibarra-Bahena, J., Romero, R. J., Velazquez-Avelar, L., Valdez-Morales, C. V., & Galindo-Luna, Y. R. (2015). Experimental thermodynamic evaluation for a single stage heat transformer prototype build with commercial PHEs. Applied Thermal Engineering, 75, 1262-1270.

Jakob, U., Eicker, U., Schneider, D., Taki, A. H., & Cook, M. J. (2008). Simulation and experimental investigation into diffusion absorption cooling machines for air-conditioning applications. Applied thermal engineering, 28(10), 1138-1150.

Khan, T. S., Khan, M. S., Chyu, M. C., & Ayub, Z. H. (2012a). Experimental investigation of evaporation heat transfer and pressure drop of ammonia in a 60 chevron plate heat exchanger. International journal of refrigeration, 35(2), 336-348.

Khan, M. S., Khan, T. S., Chyu, M. C., & Ayub, Z. H. (2012b). Experimental investigation of evaporation heat transfer and pressure drop of ammonia in a 30 chevron plate heat exchanger. International journal of refrigeration, 35(6), 1757-1765.

Lizarte, R., Izquierdo, M., Marcos, J. D., & Palacios, E. (2012). An innovative solar-driven directly air-cooled LiBr–H 2 O absorption chiller prototype for residential use. Energy and Buildings, 47, 1-11.

Lizarte, R., Izquierdo, M., Marcos, J. D., & Palacios, E. (2013). Experimental comparison of two solar-driven air-cooled LiBr/H 2 O absorption chillers: indirect versus direct air-cooled system. Energy and Buildings, 62, 323-334.

Llamas, S. U., Herrera, J. V., Cuevas, R., Gómez, V. H., García-Valladares, O., Cerezo, J., & Best, R. (2007, October). Development of a small capacity ammonia-lithium nitrate absorption refrigeration system. In 2nd Int Conference on Solar Air-Conditioning, Tarragona (pp. 470-475).

Llamas-Guillén, S. U., Cuevas, R., Best, R., & Gómez, V. H. (2014). Experimental results of a direct air-cooled ammonia–lithium nitrate absorption refrigeration system. Applied Thermal Engineering, 67(1), 362-369.

Moreno-Quintanar, G., Rivera, W., & Best, R. (2012). Comparison of the experimental evaluation of a solar intermittent refrigeration system for ice production operating with the mixtures $NH_3/LiNO_3$ and $NH_3/LiNO_3/H_2O$. Renewable energy, 38(1), 62-68.

Qu, M., Yin, H., & Archer, D. H. (2010). A solar thermal cooling and heating system for a building: experimental and model based performance analysis and design. *Solar Energy*, *84*(2), 166-182.

Rivera, W., Moreno-Quintanar, G., Rivera, C. O., Best, R., & Martínez, F. (2011). Evaluation of a solar intermittent refrigeration system for ice production operating with ammonia/lithium nitrate. Solar Energy, 85(1), 38-45.

Stasiek, J. A. (1998). Experimental studies of heat transfer and fluid flow across corrugated-undulated heat exchanger surfaces. International Journal of Heat and Mass Transfer, 41(6-7), 899-914.

Statistics, I. E. A. (2011). CO2 emissions from fuel combustion-highlights. *IEA, Paris http://www. iea. org/co2highlights/co2highlights. pdf. Cited July*.

Venegas, M., Rodríguez-Hidalgo, M. C., Salgado, R., Lecuona, A., Rodríguez, P., & Gutiérrez, G. (2011). Experimental diagnosis of the influence of operational variables on the performance of a solar absorption cooling system. Applied Energy, 88(4), 1447-1454.

Yin, Y. L., Zhai, X. Q., & Wang, R. Z. (2013). Experimental investigation and performance analysis of a mini-type solar absorption cooling system. *Applied Thermal Engineering*, *59*(1), 267-277.

Zacarías, A., Venegas, M., Lecuona, A., & Ventas, R. (2013). Experimental evaluation of ammonia adiabatic absorption into ammonia–lithium nitrate solution using a fog jet nozzle. Applied Thermal Engineering, 50(1), 781-790.

Zamora, M., Bourouis, M., Coronas, A., & Valles, M. (2014). Pre-industrial development and experimental characterization of new air-cooled and water-cooled ammonia/lithium nitrate absorption chillers. International journal of refrigeration, 45, 189-197.

Zamora, M., Bourouis, M., Coronas, A., & Vallès, M. (2015). Part-load characteristics of a new ammonia/lithium nitrate absorption chiller. International Journal of Refrigeration, 56, 43-51.

7. Appendix

Nomenclature

Parameter	Symbol	Units
Coefficient of performance	COP	dimensionless
Thermal power	$\dot{Q}$	kW
Mechanical power	$\dot{W}$	kW
Mass flow rate	$\dot{m}$	Kg/s
Specific enthalpy	h	kJ/kg
Temperature	T	°C

Subscripts

Reference	Symbol
Internal	int
Evaporator	e
Condenser	c
Generator	g
Absorber	a
Economizer	ec
Input	i
Output	o
Refrigerant	ref
Diluted/weak solution	weak
Concentrated/strong solution	strong
Water	w